Journal of the Less-Common Metals, 160 (1990) 171–180

THE CRYSTAL STRUCTURE AND THE MAGNETIC ORDER OF $U_{14}Au_{51}$

A. DOMMANN, H. R. OTT* and F. HULLIGER

Laboratorium für Festkörperphysik, ETH, CH-8093 Zürich (Switzerland)

P. FISCHER

Labor für Neutronenstreuung, ETH, CH-5232 Villigen PSI (Switzerland)

(Received September 16, 1989)

Summary

The crystal structure of $U_{14}Au_{51}$ at 295, 30 and 11 K and its magnetic structure at 11 K were determined by means of neutron diffraction, using the Rietveld powder method. The crystal structure is of the hexagonal $Gd_{14}Ag_{51}$ type (space group $P6/m$) over the whole temperature range from 11 to 295 K. Below the Néel temperature $T_N = 22$ K each set of uranium atoms at the positions 6j and 6k forms an antiferromagnetic sublattice, corresponding to the Shubnikov space group $P6'/m$. The ordered magnetic moments $\mu_{U1} = 0.5(3)\ \mu_B$ and $\mu_{U2} = 1.6(3)\ \mu_B$ at saturation are oriented parallel to the c axis. The U3 atoms in positions 2e do not contribute to the magnetic ordering. The relatively short U3–U3 distance is suggestive of 5f-electron energy-band formation.

1. Introduction

We recently described the phases occurring in the binary system U–Au [1]. Our interest in heavy-electron systems and also in a γ value of 260 mJ K^{-1} mol^{-1} reported for "UAu_3" [2] had initiated this investigation and led to our work on low temperature properties [3]. In ref. 1 it was concluded that the compounds U_2Au_3 and UAu_3 reported in a phase diagram [4] are in fact UAu_2 and $U_{14}Au_{51}$, both with hexagonal lattice symmetry, the former crystallizing in the $CeCd_2$-type structure and the latter in the $Gd_{14}Ag_{51}$ type [5]. The structural data for $U_{14}Au_{51}$ at room temperature were determined by means of a Rietveld analysis of the X-ray powder diffraction intensities [1]. The phase diagram was subsequently corrected by Palenzona and Cirafici [6]. Since UAu_2 revealed a weak temperature-independent paramagnetism between 1.5 and 300 K, we concentrated our investigations on $U_{14}Au_{51}$ [3], which shows a Curie–Weiss type susceptibility with an anomaly at 22 K, indicating antiferromagnetic ordering. Specific heat data also revealed a small

*Also at: Paul Scherrer Institut, CH-5232 Villigen PSI, Switzerland.

0022-5088/90/$3.50

anomaly at 22 K, and the formation of a heavy-electron state below 4 K. In the following we report on the results of our low temperature neutron investigations.

2. Experimental details

Polycrystalline samples of $U_{14}Au_{51}$ were prepared as described in ref. [3]. Under the microscope the polycrystalline samples appeared to be homogeneous and no lines attributable to foreign phases were detected on the X-ray diffraction patterns.

Powder neutron-diffraction measurements were performed on the multi-detector powder diffractometer DMC and on the double-axis spectrometer at the reactor Saphir (PSI). In order to determine both the positional parameters of the $Gd_{14}Ag_{51}$-type crystal structure and the arrangement of the magnetic moments, measurements were made at 295, 30 and 11 K. The neutron wavelength $\lambda = 1.706$ Å was chosen because it offered optimal intensity and resolution. Our powder sample was kept in an annular vanadium cylinder of 5 mm outer and 4 mm inner radius and 50 mm height. The diffraction patterns were measured on the DMC diffractometer with 400 channels in the "high-intensity mode" (no primary collimation). Measurements were taken in the scattering-angle ranges $2\vartheta = 7°-87°$ at 11 and 30 K and 7°–110° at 295 K, with a step width $\delta(2\vartheta) = 0.1°$. The absorption correction was based on a transmission measurement which yielded an absorption coefficient $\mu_{obs} = 2.88$ cm^{-1} at $\lambda = 1.706$ Å. The diffraction diagrams were analyzed by the Rietveld profile method, using relativistic magnetic form factors for U^{4+} in the dipole approximation. As starting parameters we used the room temperature parameters for $U_{14}Au_{51}$ deduced from X-ray diffraction measurements [1]. With neutron diffraction employed here we achieved a distinct improvement in the accuracy of the positional parameters as a consequence of the absence of X-ray fluorescence, the less severe absorption and the larger 2ϑ range. However, the preferred orientation of the crystallites, and the asymmetric peaks and diffuse background still posed some problems for the analysis of the neutron diffraction data. As an example we present the diffraction pattern at 30 K in Fig. 1.

The magnetic contribution to the diffraction intensities needed for the derivation of the magnetic structure was approximated by the difference between the diagrams obtained at 11 and 30 K (see Fig. 2). Because of the large absorption, the counting statistics for the uniformly weak magnetic contributions (the largest magnetic contribution, met in the (101) reflection, was only 2.5% of the strongest nuclear peak (140), with the background subtracted) remained rather limited. To verify our model we also measured the temperature dependence of the intensities of the (101), (110) and (001) reflections on the two-axis spectrometer with $\lambda = 2.33$ Å. The data points in Fig. 3 were obtained by subtracting the corresponding integral intensity measured at 26 K, which is safely above the Néel point, from the integral intensities measured at different temperatures below the Néel point. Moreover, the intensities from above the Néel temperature were corrected for the paramagnetic background signal which was of the same order of magnitude as the magnetic Bragg intensities. The background intensity was approximately 120 000

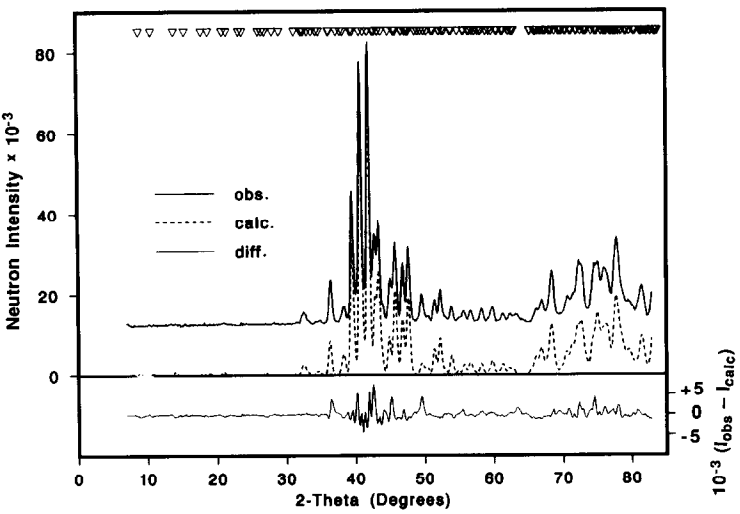

Fig. 1. Observed (line) and calculated (dashed) neutron diffraction patterns in the paramagnetic state at 30 K; the bottom curve represents the difference between calculated and observed intensities; Bragg peak positions are represented by triangles on top.

counts whereas the magnetic contributions in the ordered state were never greater than 5000 counts, which is less than 5%. The magnetic contribution to the (101) peak was about 50% whereas the (110) reflection was almost purely (99.7%) magnetic. Within the error limits we were unable to detect any magnetic contribution to the (001) and the (002) intensities, an observation which is crucial for determining the magnetic space group. A puzzling result of our intensity evaluations is the different temperature dependence of the magnetization function of the (101) and (110) peaks. The magnetic intensity of the (101) peak behaves normally, as expected for a second-order transition, in marked contrast with the (110) peak (see Fig. 3). Taking into account the large error bars of the data points, however, we must be cautious in drawing conclusions.

3. Derivation of the magnetic structure

The numerical results of the nuclear structure refinement on $U_{14}Au_{51}$ at 295 and 30 K are given in Fig. 1 and Table 1. The profile analysis of the nuclear intensities confirms the $Gd_{14}Ag_{51}$-type crystal structure reported earlier [1]. The largest discrepancies occur for the uranium atoms whose positions should now, however, be considerably more accurate. The reported standard deviations refer to the statistical errors only, not to the unknown systematic errors which are different for the X-ray and the neutron diffraction measurements.

On the basis of our physical measurements and by analogy with the magnetic structure reported for the rare-earth–gold compounds $Ln_{14}Au_{51}$ [7], we had first assumed a similar model for the magnetic structure of $U_{14}Au_{51}$ [3], but this turned out to be too simple. We had observed that the magnetic susceptibility between 25

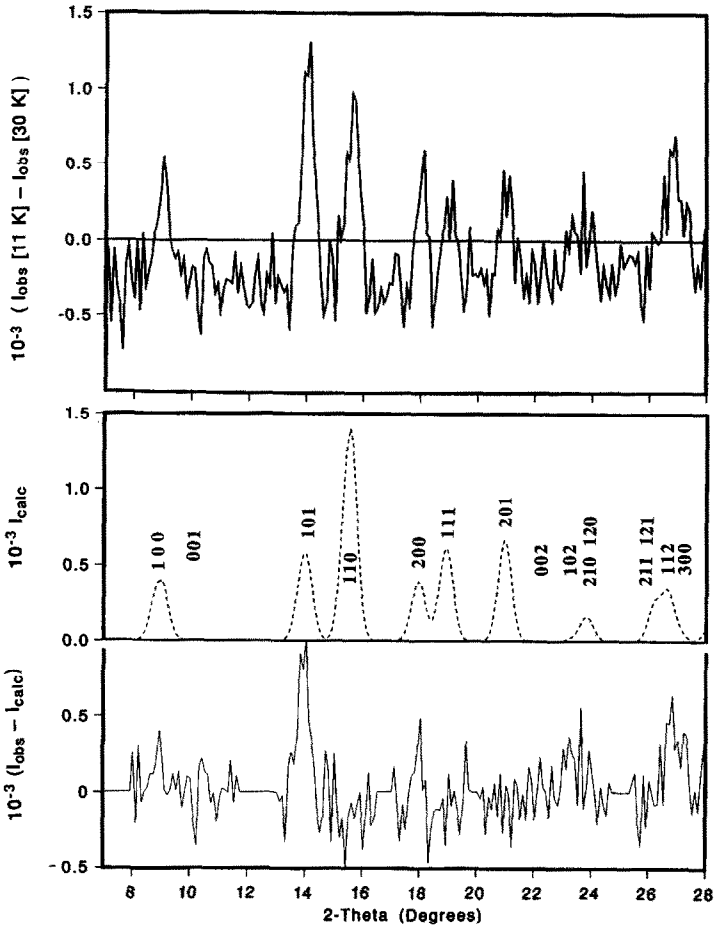

Fig. 2. Difference between the 11 K and the 30 K diagram, corresponding to magnetic neutron intensities: the dominant peaks are indexed; the background intensity is below zero owing to the vanishing paramagnetic disorder intensity in the magnetically ordered state; the fact that the intensity calculated for the (101) reflection is too small is probably due to preferred orientation or due to the inaccuracy of the underlying nuclear model.

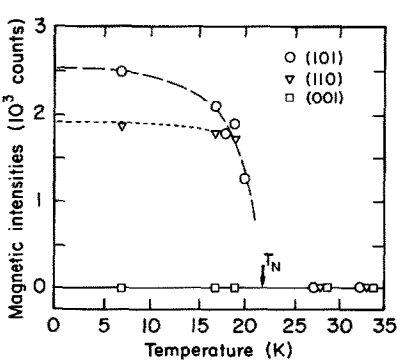

Fig. 3. Temperature dependence of magnetic peak intensities of the (101), (110) and (001) reflections: the lines are drawn as a guide to the eye; the large error bars are omitted for clarity (ΔInt 20–25 counts, ΔT 2–3 K).

TABLE 1

The nuclear structure of $Gd_{14}Ag_{51}$-type $U_{14}Au_{51}$ at 295, 30 and 11 K, and the magnetic structure at 11 K[a]

Atom	*Site*	*x*	*y*	*z*	B (Å^2)	μ_z (μ_B)
U1	6(k)	0.138(2)	0.463(2)	1/2	3.6(6)	
		0.138(2)	0.461(2)	1/2	1.6(3)	
		0.137(5)	0.460(5)	1/2	0.9(4)	0.5(3)
U2	6(j)	0.395(2)	0.109(2)	0	1.4(4)	
		0.398(2)	0.109(2)	0	1.6(3)	
		0.399(5)	0.109(5)	0	0.9(4)	1.8(3)
U3	2(e)	0	0	0.298(3)	0.8(8)	
		0	0	0.304(3)	1.0(4)	
		0	0	0.306(5)	0.7(4)	—[d]
Au1	12(l)	0.073(1)	0.265(1)	0.234(1)	0.5(3)	
		0.073(1)	0.265(1)	0.240(2)		
		0.072(6)	0.265(6)	0.242(6)		
Au2	12(l)	0.118(1)	0.493(1)	0.144(1)	1.0(3)	
		0.116(1)	0.494(1)	0.146(2)		
		0.116(6)	0.494(5)	0.146(5)		
Au3	12(l)	0.442(1)	0.104(1)	0.335(2)	1.3(3)	
		0.443(1)	0.102(1)	0.336(2)		
		0.443(6)	0.102(5)	0.336(4)		
Au4	6(k)	0.234(2)	0.052(2)	1/2	0.4(4)	
		0.231(2)	0.049(2)	1/2		
		0.232(5)	0.051(5)	1/2		
Au5[b]	6(j)	−0.025(4)	0.100(4)	0	1.2(8)	
Au5[c]		−0.022(4)	0.101(4)	0		
Au5[c]		−0.022(7)	0.098(7)	0		
Au6	4(h)	1/3	2/3	0.309(2)	0.4(4)	
		1/3	2/3	0.311(3)		
		1/3	2/3	0.312(5)		
Au7	2(c)	1/3	2/3	0	0.4(4)	
		1/3	2/3	0		
		1/3	2/3	0		

[a] d_x is the X-ray density and B is the isotropic temperature factor. R_n, R_m and R_{wp} are the reliability factors based on the integrated nuclear, the magnetic and the weighted profile intensities respectively. R_{exp} is the expected value related to the statistical accuracy of the data, and $\chi^2 = (R_{wp}/R_{exp})^2$. $\mu = (0, 0, \mu_z)$ is the absolute value of the ordered magnetic moment per atom. The estimated statistical error of the last digit is added in parentheses.

The three sets of data for each crystallographic position refer to the three temperatures, 295, 30 (paramagnetic state, space group $P6/m$ (no. 175), $Z = 1$, Pearson symbol hP68) and 11 K (antiferromagnetic state, Shubnikov space group $P6'/m$).

$T = 295$ K: $a = 12.6521(5)$ Å; $c = 9.1381(5)$ Å; $V = 1266.8(8)$ Å^3; $d_x = 17.54(2)$ g cm^{-3} [1]. $T = 30$ and 11 K: $a = 12.615(5)$ Å; $c = 9.118(5)$ Å; $V = 1257(2)$ Å^3; $d_x = 17.68(3)$ g cm^{-3}.

$T = 295$ K: $R_{wp} = 0.062$; $R_{exp} = 0.025$; $\chi^2 = 6.1$; $R_n = 0.043$. $T = 30$ K: $R_{wp} = 0.137$; $R_{exp} = 0.025$; $\chi^2 = 30$; $R_n = 0.095$. $T = 11$ K: $R_{wp} = 0.157$; $R_{exp} = 0.025$; $\chi^2 = 39$; $R_n = 0.15$; $R_m = 0.25$.

[b] Occupation number 0.50(2).

[c] Occupation number 1/2 (assumed fix).

[d] Zero owing to symmetry.

and 985 K obeys a Curie–Weiss law fairly well, with $\theta_p = -100$ K [3], showing virtually no influence of any crystalline electric field. From the slope we derived an effective magnetic moment of 3.32 μ_B/U atom. However, the sites of the uranium atoms in this structure are not equivalent. In particular, the short U3–U3 distance may allow the formation of a 5f-electron energy band by direct overlap of the corresponding wave functions. Postulating that magnetic moments are defined and well localized only on the remaining 6 U1 and 6 U2 atoms we end up with an average effective moment of 3.56 μ_B/U atom for U1 and U2, which corresponds rather well to the values expected for both U^{3+} and U^{4+}, *i.e.* 3.58 and 3.62 μ_B respectively (assuming L–S coupling). A maximum in the magnetic susceptibility $\chi(T)$ as well as an anomaly in the specific heat $c_p(T)$ both indicate the onset of antiferromagnetic ordering, as was mentioned above.

From a preliminary neutron-diffraction run at 8 K we had concluded that the magnetic cell is identical with the nuclear cell. U1 and U2 are located on sixfold positions and each set thus could form a ferromagnetic or an antiferromagnetic sublattice. Before the present determination of the magnetic space group, the expected analogy to $Ln_{14}Au_{51}$ [7] led us to assume the first possibility [3] (corresponding to the magnetic space group $P6/m$). Calculations of the magnetic intensities with this model, however, turned out to be in disagreement with the intensities derived from our new and more accurate measurements. Our present 11 K neutron diffraction pattern confirms the absence of additional, *i.e.* purely magnetic, peaks thus reducing the remaining possibilities to the three Shubnikov space groups $P6'/m$, $P6/m'$ or $P6'/m'$ [8], indicating antiferromagnetic uranium sublattices throughout. Unfortunately, none of the three calculated diffraction patterns leads to a very good R_m value, but the best agreement with the measurements is obtained with the space group $P6'/m$ ($R_m = 0.25$, 0.57 and 0.52 respectively). In this space group U3 cannot have a moment parallel to the z axis because of the site symmetry, which is consistent with our former assumption. All model calculations in the other space groups, $P6/m'$ and $P6'/m'$, however, lead to magnetic contributions perpendicular to the z axis. The absence of any magnetic contribution to the $(00l)$ reflections at 11 K (Figs. 2 and 3) thus clearly invalidates these two possibilities. Moreover, the magnetic moments on the uranium atoms required by these models proved to be much too large (> 6 μ_B/U atom).

It is note worthy that in the magnetic structure of $U_{14}Au_{51}$ the moments of U1 and U2 came out distinctly different. Although this difference is crystallographically reasonable, we also checked a fit with equal moments, but in this case R_m was about 40% larger than in the model with unequal moments.

The results of our calculations on both the magnetic and the nuclear structure at 11 K are summarized in Table 1. Interatomic distances are listed in Table 2.

4. Discussion

Figure 4 illustrates the arrangement of the two magnetic sublattices. The two uranium subsets form spatially well-separated layers in the mirror planes of $P6/m$; the U1 atoms all are located at $z = 1/2$; the U2 atoms all lie in the basal plane, $z = 0$.

TABLE 2

Interatomic distances (calculated to beyond the coordination gap, particularly the U–U distances) in $U_{14}Au_{51}$ at 11 K

Atom[a]	*Ligand*[a]	*Distance* (Å)[b]	*Atom*	*Ligand*	*Distance* (Å)[b]
U1 (↑)	2 Au3	3.01(2)	Au2	1 Au2	2.67(2)
	2 Au6	3.07(3)		1 Au3	2.78(2)
	2 Au3	3.08(2)		1 Au1	2.80(2)
	1 Au4	3.11(2)		1 Au7	2.84(2)
	2 Au3	3.14(2)		1 Au6	2.93(2)
	1 Au4	3.19(3)		1 Au3	3.00(2)
	2 Au1	3.20(2)		1 Au2	3.01(2)
	2 Au2	3.29(2)		1 U2	3.03(2)
	1 U1 (↓)	4.06(3)[c]		1 U2	3.08(2)
	2 U1 (↑)	4.41(3)[c]		1 U2	3.27(2)
	2 U2 (↓)	5.16(3)[c]		1 U1	3.29(2)
	2 U1 (↓)	5.16(3)[c]		1 Au3	3.65(3)[c]
	2 U2 (↑)	5.33(3)[c]		1 Au2	4.02(3)[c]
	2 U3	5.46(3)[c]			
U2 (↑)	2 Au2	3.03(2)			
	2 Au2	3.08(2)	Au3	1 Au2	2.78(3)
	1 or 0 Au5	3.12(4)		1 Au4	2.84(3)
	2 Au3	3.13(2)		1 Au6	2.88(3)
	1 Au7	3.14(2)		1 Au1	2.93(2)
	2 Au1	3.27(2)		1 Au3	2.99(3)
	2 Au2	3.27(3)		1 Au2	3.00(3)
	2 Au1	3.31(3)		1 U1	3.01(3)
	0 or 1 Au5	3.87(5)[c]		1 U1	3.08(3)
	1 Au5	4.13(2)[c]		1 Au1	3.11(2)
	2 Au6	4.24(2)[c]		1 U2	3.13(3)
	2 U2 (↓)	4.51(3)[c]		1 U1	3.14(3)
	1 U2 (↓)	4.59(3)[c]		1 Au3	3.52(3)[c]
	2 U1 (↓)	5.16(3)[c]		1 Au2	3.65(3)[c]
	2 U3	5.30(3)[c]		1 Au7	4.20(3)[c]
	2 U1 (↑)	5.33(3)[c]			
	2 U2 (↑)	5.44(3)[c]	Au4	2 Au4	2.67(3)
U3	6 Au1	3.05(2)		2 Au1	2.73(3)
	6 Au5	3.12(2)		2 Au3	2.84(3)
	6 Au4	3.20(2)		2 Au1	2.86(3)
	1 U3	3.54(2)[c]		1 U1	3.11(3)
	6 U2	5.30(3)[c]		1 U1	3.19(3)
	6 U1	5.46(3)[c]		2 U3	3.21(3)
	1 U3	5.59(3)[c]		2 Au1	4.57(3)[c]
			Au5	1 Au5	2.79(3)
Au1	1 Au4	2.73(2)		2 Au1	2.87(3)
	1 Au2	2.80(2)		2 Au1	2.99(3)
	1 Au4	2.86(2)		1 U2	3.12(3)
	1 or 0 Au5	2.87(4)		2 U3	3.12(3)
	1 Au3	2.93(2)		1 U2	3.87(3)[c]
	0 or 1 Au5	2.99(2)		2 Au1	3.89(3)[c]
	2 Au1	3.00(2)		2Au1	4.06(3)[c]

TABLE 2 (*continued*)

Atom[a]	*Ligand*[a]	*Distance* (Å)[b]	*Atom*	*Ligand*	*Distance* (Å)[b]
Au1	1 U3	3.05(2)			
(*continued*)	1 Au3	3.11(2)			
	1 U1	3.20(2)			
	1 U2	3.27(2)	Au6	1 Au7	2.85(2)
	1 U2	3.31(2)		3 Au3	2.88(3)
	0 or 1 Au5	3.87(4)[c]		3 Au2	2.93(3)
	1 Au5	4.06(2)[c]		3 U1	3.07(3)
	1 Au1	4.42(2)[c]		1 Au6	3.43(3)[c]
				3 U2	4.24(3)[c]
			Au7	6 Au2	2.84(3)
				2 Au6	2.84(3)
				3 U2	3.14(3)
				6 Au3	4.20(4)[c]

[a]The relative orientation of the magnetic moments of U1 and U2 is indicated by arrows.
[b]The estimated error of the last digit is added in parentheses.
[c]Beyond the coordination gap.

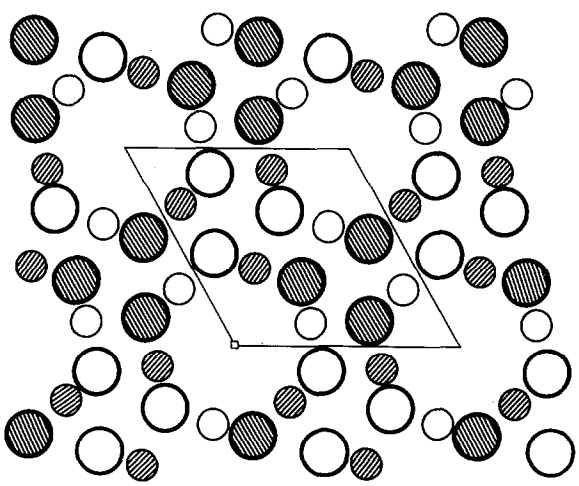

Fig. 4. The magnetic structure of $U_{14}Au_{51}$ at 11 K: the U1 atoms, which are located at $z = 1/2$, are designated by the large bold circles, while the U2 atoms in the basal plane (which actually carry the larger moments) are given by the smaller faint circles; the orientation of the magnetic moments is opposite in atoms represented by open and hatched circles.

The positions, including the magnetic moment along the c axis, are given as (see Table 1)

$$6j(z=0) \text{ and } 6k(z=1/2): \pm(x, y, \mu_z; \bar{y}, x-y, \mu_z; y-x, \bar{x}, \mu_z)$$

The values of the corresponding x and y parameters are almost interchanged. In both layers the up and down moments are located on uranium triangles centred at

(1/3, 2/3) and (2/3, 1/3), but the particular values of the x and y parameters shift the corresponding triangles into opposite corners of the unit cell. Thus the uranium triangles stacked along 1/3, 2/3, z, as well as those along 2/3, 1/3, z, show alternating orientations of their (different) magnetic moments (Fig. 4). Since the U2 triangles are centred by an Au7 atom these U2–U2 distances are fairly large (5.44 Å). In fact, the distances within the six-membered U2 rings, *i.e.* the U↑–U↓ distances, are considerably shorter than the U↑–U↑ distances within the U2↑ triangles. The U1 triangles, in contrast, appear as distinct building units: U↑–U↑ = 4.41 Å, although the distance to the neighbouring unit is even smaller; each corner atom of the U1↑ unit is as close as 4.06 Å to a U1 atom of the neighbouring U1↓ unit. The interlayer distances U1–U2 are 5.16 and 5.33 Å. These distances are different because the six-membered U1 and U2 rings (or, which is symmetry equivalent, the superposed U1↑ and U2↓ triangles) are rotated relative to each other by an angle slightly different from 30°, namely $(32.2 \pm 1.9)°$. The relative orientation of the magnetic moments of the two sublattices is determined by this difference. Our refinement demonstrates that the magnetic coupling along the shorter distance is antiferromagnetic whereas along the larger distance the orientation of the magnetic moments is necessarily ferromagnetic. The signs of the magnetic moments of both sites 6(j) and 6(k) are thus equal, and a change in the sign at one site results in a dramatic increase in R_m. Moreover, the magnetic structure appears to be fairly stable since the magnetic-field dependence of the magnetization at 1.6 K was found to be perfectly linear up to 10 T.

In this connection it may be note worthy that a partial substitution of the gold atoms by the smaller copper atoms (a complete replacement appears to be impossible under normal conditions) leads to a lower ordering temperature. For $U_{14}Cu_9Au_{42}$ [1] preliminary susceptibility and specific heat measurements indicated a Néel temperature $T_N = 16$ K.

For the isotypical rare earth phases $Ln_{14}Au_{51}$ with the heavy rare earth elements, Ikonomou *et al.* [7] assumed two ferromagnetic sublattices (neglecting the Ln3 sublattice), based on theoretical studies by Yakinthos *et al.* [9]. Since an analogy U ↔ Ln would be possible only if the lanthanide element was cerium, which, however, is a light rare earth element, the magnetic space group of the ordered $Ln_{14}Au_{51}$ and, of course, $Ln_{14}Ag_{51}$ phases must differ from that of $U_{14}Au_{51}$.

Since $U_{14}Au_{51}$ contains magnetic as well as non-magnetic uranium atoms the occurrence of superconductivity would not be too surprising. However, as our susceptibility and specific heat measurements [3] indicated, $U_{14}Au_{51}$ remains normal down to 0.1 K. Even in the non-magnetic analogs $Th_{14}Au_{51}$ and $Y_{14}Ag_{51}$ we found no indication of a superconductive transition down to 1.6 K.

Acknowledgments

We thank Stefan Siegrist (ETHZ) as well as the workshop group of LNS for technical assistance, and the Swiss National Science Foundation for financial support.

References

1 A. Dommann and F. Hulliger, *J. Less-Common Met., 141* (1988) 261.
2 Z. Fisk, G. R. Stewart, B. Batlogg and E. Bucher, unpublished; cited in G. R. Stewart, *Rev. Mod. Phys., 56* (1984) 755, Table VI.
3 H. R. Ott, E. Felder, A. Schilling, A. Dommann and F. Hulliger, *Solid State Commun., 71* (1989) 549.
4 R. W. Buzzard and J. J. Park, *J. Res. Nat. Bur. Stand., 53* (1954) 291.
5 P. Villars and L. D. Calvert, *Pearson's Handbook of Crystallographic Data for Intermetallic Phases*, Vol. 1, American Society for Metals, Metals Park, Ohio, U.S.A., 1985.
6 A. Palenzona and S. Cirafici, *J. Less-Common Met., 143* (1988) 167.
7 P. F. Ikonomou, J. K. Yakinthos and T. Anagnostopoulos, *J. Less-Common Met., 59* (1978) P51.
8 V. A. Koptsik, *Shubnikovie Gruppy—Spravochnik po Simmetrii i Fisicheskim Svoistvam Kristallicheskikh Struktur (Shubnikov groups—A Handbook on Symmetry and Physical Properties of Crystal Structures)*, Moscow University Press, Moscow, 1966, p. 123.
9 J. K. Yakinthos, T. Anagnostopoulos and P. F. Ikonomou, *J. Less-Common Met., 51* (1977) 113.